

## Thermal Transport Measurements of Individual Multiwalled Nanotubes

P. Kim,<sup>1</sup> L. Shi,<sup>2</sup> A. Majumdar,<sup>2</sup> and P. L. McEuen<sup>1,3,\*</sup>

<sup>1</sup>*Department of Physics, University of California, Berkeley, California 94720*

<sup>2</sup>*Department of Mechanical Engineering, University of California, Berkeley, California 94720*

<sup>3</sup>*Division of Materials Sciences, Lawrence Berkeley National Laboratory, Berkeley, California 94720*

(Received 1 June 2001; published 31 October 2001)

The thermal conductivity and thermoelectric power of a single carbon nanotube were measured using a microfabricated suspended device. The observed thermal conductivity is more than 3000 W/K m at room temperature, which is 2 orders of magnitude higher than the estimation from previous experiments that used macroscopic mat samples. The temperature dependence of the thermal conductivity of nanotubes exhibits a peak at 320 K due to the onset of umklapp phonon scattering. The measured thermoelectric power shows linear temperature dependence with a value of 80  $\mu\text{V/K}$  at room temperature.

DOI: 10.1103/PhysRevLett.87.215502

PACS numbers: 61.46.+w, 63.22.+m, 65.80.+n

The thermal properties of carbon nanotubes are of fundamental interest and also play a critical role in controlling the performance and stability of nanotube devices [1]. Unlike electrical and mechanical properties, which have been studied at a single nanotube level [2], the thermal properties of carbon nanotubes have not been measured at a mesoscopic scale. The specific heat, thermal conductivity, and thermoelectric power (TEP) of millimeter-sized mats of carbon nanotubes have been measured by several groups [3–13]. Although these studies have yielded a qualitative understanding of the thermal properties of these materials, there are significant disadvantages to these “bulk” measurements for understanding intrinsic thermal properties of a single nanotube. One problem is that these measurements yield an ensemble average over the different tubes in a sample. More importantly, in thermal transport measurements such as thermal conductivity and TEP, it is difficult to extract absolute values for these quantities due to the presence of numerous tube-tube junctions. These junctions are in fact the dominant barriers to thermal transport in a mat of nanotubes.

In this Letter, we present the results of mesoscopic thermal transport measurements of individual carbon nanotubes. We have developed a microfabricated suspended device hybridized with multiwalled nanotubes (MWNTs) to probe thermal transport free from a substrate contact. The observed thermal conductivity of a MWNT is 2 orders of magnitude higher than the value found in previous bulk measurements and is comparable to the theoretical expectations.

Suspended structures were fabricated on a silicon nitride/silicon oxide/silicon multilayer by electron beam and photolithography followed by metallizations and etching processes, which are described elsewhere in detail [14]. Figure 1(a) shows a representative device including two  $10\ \mu\text{m} \times 10\ \mu\text{m}$  adjacent silicon nitride membrane ( $0.5\ \mu\text{m}$  thick) islands suspended with  $200\ \mu\text{m}$  long silicon nitride beams. On each island, a Pt thin film resistor, fabricated by electron beam lithography, serves as a heater

to increase the temperature of the suspended island. These resistors are electrically connected to contact pads by the metal lines on the suspending legs. Since the resistance of the Pt resistor changes with temperature [Fig. 1(b)], they also serve as a thermometer to measure the temperature of each island [15].

Once the suspended devices were fabricated, carbon nanotubes were placed on the device and bridged the two suspended islands. Mechanical manipulation similar to

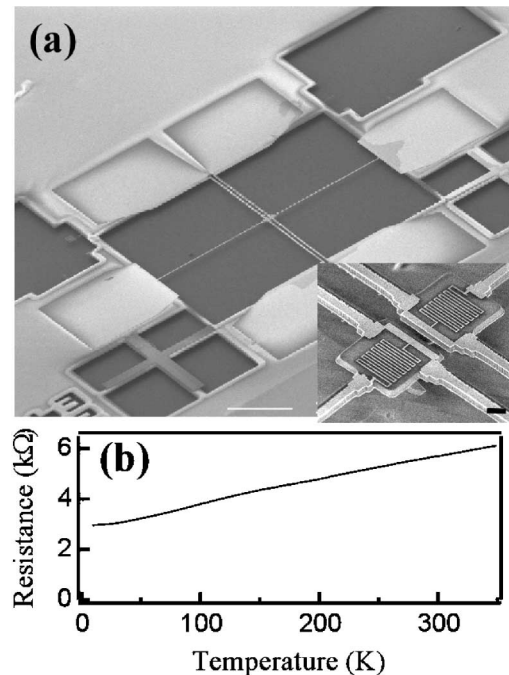


FIG. 1. (a) A large scale scanning electron microscopy (SEM) image of a microfabricated device. Two independent islands are suspended by three sets of  $250\ \mu\text{m}$  long silicon nitride legs with Pt lines that connect the microthermometer on the islands to the bonding pads. The scale bar represents  $100\ \mu\text{m}$ . Inset: Enlarged image of the suspended islands with the Pt resistors. The scale bar represents  $1\ \mu\text{m}$ . (b) The resistance of the Pt resistor over the measured temperature ranges.

that used for the fabrication of nanotube scanning probe microscopy tips [16] was used to place MWNTs on the desired part of the device. This approach routinely produces a nanotube device that can be used to measure the thermal conductivity and TEP of the bridging nanotube segment. Shown in Fig. 2 (upper inset) is an example of such a device. A small MWNT bundle forms a thermal path between two suspended islands that are otherwise thermally isolated to each other. A bias voltage applied to one of the resistors,  $R_h$ , creates joule heat and increases the temperature,  $T_h$ , of the heater island from the thermal bath temperature  $T_0$ . Under steady state, there is a heat transfer to the other island through the nanotubes, and thus the temperature,  $T_s$ , of the resistor  $R_s$  also rises. Using a simple heat transfer model (lower inset of Fig. 2), the thermal conductance of the connecting nanotubes,  $K_t$ , and the suspending legs,  $K_d$ , can readily be estimated from  $T_h = T_0 + \frac{K_d + K_t}{K_d(K_d + 2K_t)}P$  and  $T_s = T_0 + \frac{K_t}{K_d(K_d + 2K_t)}P$ , where  $P$  is the joule power applied to the resistor  $R_h$ . Figure 2 shows the temperature changes of each of the suspended islands connected by the nanotubes as a function  $P$ . From the slopes of  $R_s$  and  $R_h$  versus  $P$ , the thermal conductance of the bridging nanotubes at the temperature  $T_0$  can be computed using the above equations.

We now turn to the experimental results of thermal conductance measurement of a single MWNT. Figure 3 displays measured thermal conductance of a single MWNT with a diameter  $d = 14$  nm and the length of the bridging segment  $2.5 \mu\text{m}$ . The thermal conductance was measured in a temperature range 8–370 K [17]. It increases by several orders of magnitude as the temperature is raised, reaching a maximum of approximately  $1.6 \times 10^{-7}$  W/K near room temperature before decreasing again at higher temperatures.

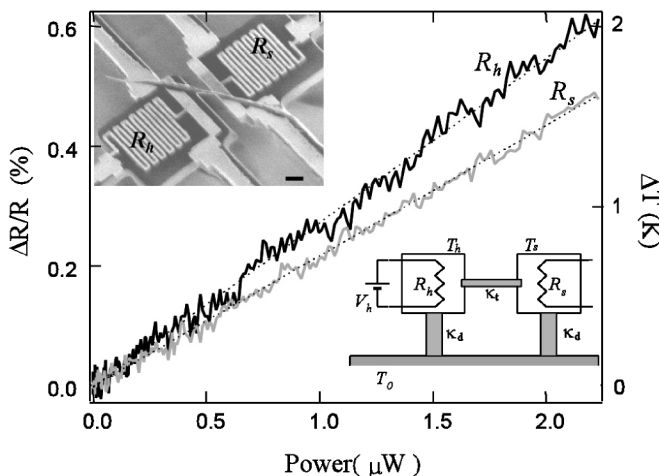


FIG. 2. The change of resistance of the heater resistor ( $R_h$ ) and sensor resistor ( $R_s$ ) as a function of the applied power to the heater resistor. Upper inset: SEM image of the suspended islands with a MWNT bundle across the device. The scale bar represents  $1 \mu\text{m}$ . Lower inset: A schematic heat flow model of the device.

The measured thermal conductance includes the thermal conductance of the junction between the MWNT and the suspended islands in addition to the intrinsic thermal conductance of the MWNT itself. From our separate study of scanning thermal microscopy on a self-heated MWNT [18], we have estimated the thermal conductance of the junction at room temperature; the heat flow rate from a unit length of the tube to a metal electrode at a given unit junction temperature difference was found to be  $\sim 0.5$  W/mK. Considering the contact length of the MWNT to the electrodes on the islands is  $\sim 1 \mu\text{m}$ ; the junction thermal conductance is  $\sim 5 \times 10^{-7}$  W/K at room temperature. Since the total measured thermal conductance is  $1.6 \times 10^{-7}$  W/K, this suggests that the intrinsic thermal conductance of the tube is the major part of measured thermal conductance.

To estimate thermal conductivity from this measured thermal conductance, we have to consider the geometric factors of the MWNT and the anisotropic nature of thermal conductivity. The outer walls of the MWNT that make good thermal contacts to a thermal bath give more contribution in thermal transport than the inner walls, and the ratio of axial to radial thermal conductivity may influence the conversion of thermal conductance to thermal conductivity. In the following, however, we simply estimate the thermal conductivity neglecting the junction thermal conductance and assuming a solid isotropic material to correct geometric factors. This simplification implies that the thermal conductivity reported in this Letter is a lower bound of

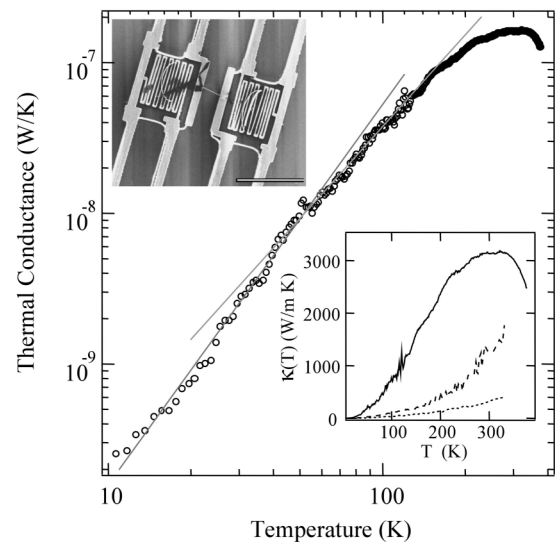


FIG. 3. The thermal conductance of an individual MWNT of a diameter 14 nm. The solid lines represent linear fits of the data in a logarithmic scale at different temperature ranges. The slopes of the line fits are 2.50 and 2.01, respectively. Lower inset: Solid line represents  $\kappa(T)$  of an individual MWNT ( $d = 14$  nm). Broken and dotted lines represent small ( $d = 80$  nm) and large bundles ( $d = 200$  nm) of MWNTs, respectively. Upper inset: SEM image of the suspended islands with the individual MWNT. The scale bar represents  $10 \mu\text{m}$ .

the intrinsic axial thermal conductivity of a MWNT. Further study to analyze the contribution of individual layers of MWNTs [19] in the thermal transport should elucidate this important issue in the future.

Shown in the lower inset of Fig. 3 is the temperature dependent thermal conductivity,  $\kappa(T)$  (solid line). This result shows remarkable differences from the previous bulk measurements as described below. First, the room temperature value of  $\kappa(T)$  is over 3000 W/m K [20], whereas the previous bulk measurement on a MWNT mat using a self-heating method estimates only 20 W/m K [4]. Note that our observed value is also an order of magnitude higher than that of an aligned single walled nanotube (SWNT) sample (250 W/m K) [7] but comparable to the recent theoretical expectations of 3000–6000 W/m K [21–23]. This large difference between single-tube and bulk measurements suggests that numerous highly resistive thermal junctions between the tubes largely dominate the thermal transport in mat samples. Second,  $\kappa(T)$  shows interesting temperature dependent behavior that was absent in bulk measurement. At low temperatures,  $8 < T < 50$  K,  $\kappa(T)$  increases following a power law with an exponent 2.50. In the intermediate temperature range ( $50 < T < 150$  K),  $\kappa(T)$  increases almost quadratically in  $T$  [i.e.,  $\kappa(T) \sim T^2$ ]. Above this temperature range,  $\kappa(T)$  deviates from quadratic temperature dependence and has a peak at 320 K. Beyond this peak,  $\kappa(T)$  decreases rapidly. For a comparison, we also show  $\kappa(T)$  of a small ( $d = 80$  nm) and a large ( $d = 200$  nm) bundle of MWNTs in the figure (broken and dotted lines, respectively). As the diameter of a MWNT bundle increases, the aforementioned features in  $\kappa(T)$  quickly disappear, and  $\kappa(T)$  becomes similar to the bulk measurement on a mat sample [4].

We now seek to understand the physics behind the observed behavior of the thermal conductivity. In a simple model [24], the phonon thermal conductivity can be written as  $\kappa = \sum_p C_p v_p l_p$ , where  $C_p$ ,  $v_p$ , and  $l_p$  is the specific heat capacity, the phonon group velocity, and the mean free path of phonon mode  $p$ . The phonon mean free path consists of two contributions:  $l^{-1} = l_{st}^{-1} + l_{um}^{-1}$  where  $l_{st}$  and  $l_{um}$  are static and umklapp scattering lengths, respectively. At low temperatures, the umklapp scattering freezes out,  $l = l_{st}$ , and thus  $\kappa(T)$  simply follows the temperature dependence of  $C_p$ 's. For MWNTs, below the Debye temperature of interlayer phonon mode  $\Theta_{\perp}$ ,  $\kappa(T)$  has slight three dimensional nature, and  $\kappa(T) \sim T^{2.5}$  as observed in graphite single crystals [25]. As  $T > \Theta_{\perp}$ , the interlayer phonon modes are fully occupied, and  $\kappa(T) \sim T^2$ , indicative of the two dimensional nature of thermal conduction in a MWNT [26]. From this crossover behavior of  $\kappa(T)$ , we estimate  $\Theta_{\perp} = 50$  K. This value is comparable to the value obtained by a measurement of specific heat of MWNT [4].

As  $T$  increases further, the strong phonon-phonon umklapp scattering becomes more effective as higher energy phonons are thermally populated. Once  $l_{st} > l_{um}$ ,  $\kappa(T)$

decreases as  $T$  increases due to rapidly decreasing  $l_{um}$ . At the peak value of  $\kappa(T)$ , where  $l_{st} \sim l_{um}$  ( $T = 320$  K), we can estimate the  $T$ -independent  $l_{st} \sim 500$  nm for the MWNT. Note that this value is an order of magnitude higher than previous estimations from bulk measurements [7] and is comparable to the length of the measured MWNT (2.5  $\mu$ m). Thus below room temperature where the phonon-phonon umklapp scattering is minimal, phonons have only a few scattering events between the thermal reservoirs, and the phonon transport is “nearly” ballistic. This remarkable behavior was not seen in the bulk experiments, possibly due to additional extrinsic phonon scattering mechanisms such as tube-tube interactions.

In addition to the probing of the thermal conductivity, the same suspended device can be used to measure the thermoelectric power of the nanotube. The two independent electrodes that contact the ends of MWNTs on each suspended island serve to measure the electrical potential difference across the tube when joule heating in  $R_h$  creates a temperature gradient across the tube. Shown in the inset of Fig. 4 is the relation of the thermoelectric voltage of the suspended MWNT to the joule heating in  $R_h$ . Since the temperature difference can be computed from an independent measurement of  $R_h$  and  $R_s$ , the TEP of the single MWNT is obtained from the slope of this curve. The observed temperature dependent TEP of MWNTs (Fig. 4) shows a linear  $T$  dependence, with room temperature value 80  $\mu$ V/K. The linear  $T$  dependence is expected from a theory for metallic and doped semiconducting nanotubes [9,13], and the positive sign indicates a holelike major carrier [27]. It is worth noting that this observed TEP is markedly different from the previous bulk measurement that exhibited somewhat smaller TEP and deviations from a linear  $T$  dependence [8]. Again, we believe that the numerous unknown tube-tube junctions in the “mat” sample may produce these differences, and that a mesoscopic

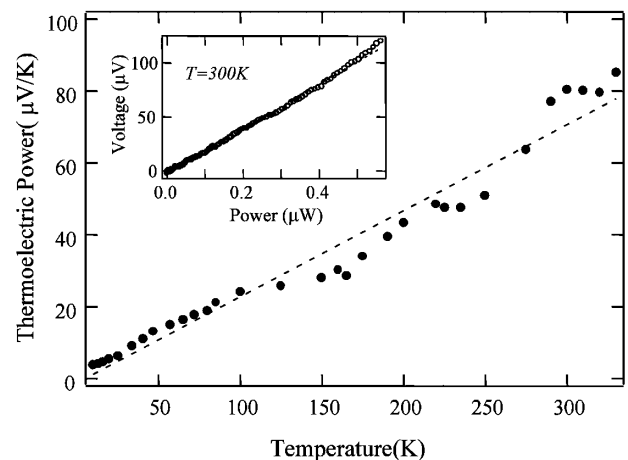


FIG. 4. The measured thermoelectric power (solid circles) and a linear fit (broken lines). Inset: The thermoelectric voltage versus the power applied to the heater resistor at 300 K. The broken line corresponds to a linear fit.

measurement of a single tube is necessary to properly probe the intrinsic TEP of nanotubes.

In conclusion, we have presented, for the first time, mesoscopic thermal transport measurements of carbon nanotubes. The observed thermal conductivity of a MWNT is more than 3000 W/mK at room temperature and the phonon mean free path is  $\sim 500$  nm. The temperature dependence of the thermal conductivity shows a peak at 320 K due to the onset of umklapp phonon scattering. The thermoelectric power shows an expected linear  $T$  dependence, which was absent in previous bulk measurements. The experimental techniques reported here should be readily applicable to other nanoscale materials to study their thermal properties.

Of particular interest are SWNTs, where the quantization of the phonon degrees of freedom has been shown to modify the heat capacity [5] and should lead to thermal conductance quantization [15] at low temperatures. Experiments attempting to measure this are under way [28].

The authors wish to thank J. Hone, D. Li, S. Jhi, Y.-K. Kwon, and D. Tomanek for helpful discussions. We also thank A. Rinzler and R. E. Smalley for supplying the nanotube materials. L. S. and A. M. would like to acknowledge the support of the DOE (Basic Energy Sciences, Engineering Division). P. K. and P. L. M. were supported by the DOE (Basic Energy Sciences, Materials Sciences Division, and the  $sp^2$  Materials Initiative).

---

\*Present address: Laboratory of Atomic and Solid State Physics, Cornell University, Ithaca, NY 14853.

- [1] M. S. Dresselhaus, G. Dresselhaus, and P. C. Eklund, *Science of Fullerenes and Carbon Nanotubes* (Academic, San Diego, 1996).
- [2] C. Dekker, *Phys. Today* **52**, No. 5, 22 (1999).
- [3] A. Mizel, L. X. Benedict, M. L. Cohen, S. G. Louie, A. Zettl, N. K. Budraa, and W. P. Beyermann, *Phys. Rev. B* **60**, 3264 (1999).
- [4] W. Yi, L. Lu, Z. Dian-lin, Z. W. Pan, and S. S. Xie, *Phys. Rev. B* **59**, R9015 (1999).
- [5] J. Hone, B. Batlogg, Z. Benes, A. T. Johnson, and J. E. Fischer, *Science* **289**, 1730 (2000).
- [6] J. Hone, M. Whitney, C. Piskoti, and A. Zettl, *Phys. Rev. B* **59**, R2514 (1999).
- [7] J. Hone, M. C. Llaguno, N. M. Nemes, A. T. Johnson, J. E. Fischer, D. A. Walters, M. J. Casavant, J. Schmidt, and R. E. Smalley, *Appl. Phys. Lett.* **77**, 666 (2000).
- [8] M. Tian, F. Li, L. Chen, Z. Mao, and Y. Zhang, *Phys. Rev. B* **58**, 1166 (1998).
- [9] J. Hone, I. Ellwood, M. Munro, A. Mizel, M. L. Cohen, A. Zettl, A. G. Rinzler, and R. E. Smalley, *Phys. Rev. Lett.* **80**, 1042 (1998).
- [10] E. S. Choi, D. S. Suh, G. T. Kim, D. C. Kim, Y. W. Park, K. Liu, G. Duesberg, and S. Roth, *Synth. Met.* **103**, 2504 (1999).
- [11] L. Grigorian, G. U. Sumanasekera, A. L. Loper, S. L. Fang, J. L. Allen, and P. C. Eklund, *Phys. Rev. B* **60**, R11309 (1999).
- [12] P. G. Collins, K. Bradley, M. Ishigami, and A. Zettl, *Science* **287**, 1801 (2000).
- [13] K. Bradley, S. H. Jhi, P. G. Collins, J. Hone, M. L. Cohen, S. G. Louie, and A. Zettl, *Phys. Rev. Lett.* **85**, 4361 (2000).
- [14] L. Shi, Ph.D. thesis, University of California, Berkeley, 2001.
- [15] K. Schwab, E. A. Henriksen, J. M. Worlock, and M. L. Roukes, *Nature (London)* **404**, 974 (2000).
- [16] H. Dai, J. H. Hafner, A. G. Rinzler, D. T. Colbert, and R. E. Smalley, *Nature (London)* **384**, 147 (1996).
- [17] Below 8 K, both  $R_s$  and  $R_h$  become saturated due to the impurity scattering and cannot be used for a temperature sensor. To insure that the measurement remains in the linear response regime,  $P$  was limited to make  $T_h - T_0 < 1$  K during the measurement.
- [18] L. Shi, P. Kim, A. Bachtold, S. Plasunov, A. Majumdar, and P. L. McEuen (unpublished).
- [19] P. G. Collins, M. Hersam, M. Arnold, R. Martel, and Ph. Avouris, *Phys. Rev. Lett.* **86**, 3128 (2000); P. Collins, M. Hersam, M. Arnold, and Ph. Avouris, *Science* **292**, 706 (2001).
- [20] The major uncertainty of  $\kappa$  arises from the uncertainty in the diameter measurement. A high resolution SEM is used to determine the diameter of MWNT to be 14 nm while the resolution limit is 2 nm.
- [21] S. Berber, Y. K. Kwon, and D. Tomanek, *Phys. Rev. Lett.* **84**, 4613 (2000).
- [22] J. Che, T. Cagin, and W. A. Goddard, *Nanotechnology* **11**, 65 (2000).
- [23] M. Osman and D. Srivastava, *Nanotechnology* **12**, 21 (2001).
- [24] The electrical contribution of thermal conductivity,  $\kappa_{el}$ , can be estimated using Wiedemann-Franz law. From the experimentally obtained electrical resistance of the MWNT,  $\kappa_{el}/\kappa \sim 10^{-3}$  at room temperature, and this ratio becomes even smaller at the lower temperatures.
- [25] B. T. Kelly, *Physics of Graphite* (Applied Science Publishers, London, 1981).
- [26] The thermal effects of one dimensional phonon quantization in a nanotube should be measurable as  $T < T_{1D} = hv/k_B R$ , where  $h$  is the Planck constant,  $k_B$  is the Boltzmann constant, and  $R$  is the radius of the nanotube. For a MWNT,  $T_{1D}$  is estimated to be  $\sim 1$  K. Above this temperature, phonon transport in a MWNT essentially behaves as in a two dimensional graphene sheet.
- [27] In a recent study, Collins *et al.* (Ref. [12]) demonstrated that the TEP of nanotubes is sensitive to gas adsorption and resulting electrical doping. The MWNTs used in our experiments were exposed in air and presumably doped with oxygen.
- [28] To date, we have not been able to successfully apply the manipulation technique described in [16] to the deposition of individual SWNTs, and other techniques are being attempted.